Int. J. Multiphase Flow Vol. 17, No. 2, pp. 247–265, 1991
Printed in Great Britain

0301-9322/91 $3.00 + 0.00
Pergamon Press/Elsevier

STOCHASTIC MODELLING OF THE EFFECTS OF LIQUID DROPLET COLLISIONS IN IMPINGING STREAMS ABSORBERS AND COMBUSTORS

A. KITRON,[1] T. ELPERIN[2,3] and A. TAMIR[1]

Department of [1]Chemical Engineering and [2]Mechanical Engineering and
[3]Pearlstone Center for Aeronautical Engineering Studies, Ben-Gurion University of the Negev,
Beer-Sheva 84120, Israel

(Received 29 January 1990; in revised form 23 October 1990)

Abstract— A stochastic model based on the Boltzmann kinetic equation and employing the comprehensive treatment of the dynamics of binary droplet collisions is suggested to describe the droplet size and spatial distribution in dense spray. The model is valid for highly non-equilibrium impinging sprays in which the inertia of the droplets is very high and dynamic coupling with the gas is low. A Monte Carlo simulation procedure is developed for the solution of the kinetic equation. A model is used to analyse the absorption of a gas in a liquid spray in an impinging streams absorber. It is demonstrated that droplet collisions result mainly in coalescence, and reduce the overall droplet concentration and the interphase area in the reactor. The results of the analysis of the vaporization of a pentane spray in an impinging streams combustor are presented. It is shown that while droplet collisions reduce the vaporization rate by deflecting droplets out of the reactor and by coalescence, collision-induced fragmentation strongly affects the droplet size distribution and increases the fuel vaporization rate. The obtained results indicate that in the high velocity combustion of light fuels the collision-induced fragmentation of fuel droplets has a profound effect on the droplet size and spatial distribution.

Key Words: impinging jets, spray combustion, binary droplet collisions, coalescence and fragmentation, Boltzmann equation, Monte Carlo method

1. INTRODUCTION

Spray systems are commonly used in processes involving gas–liquid operations. The rate of convective transfer processes such as absorption, desorption and vaporization, is an increasing function of the relative velocity between the phases. In sprays, however, the relative velocity between the carrying gas and the liquid droplets is usually small. In order to compensate for the low transfer rates, longer droplet residence times are required, necessitating longer batch durations or the use of larger size equipment.

Impinging streams reactors, first proposed by Elperin (1961), have been suggested as a method for enhancing mass and heat transfer processes in flowing gas–liquid or gas–solid suspensions. In such reactors, two droplet-laden gaseous jets flowing in opposite directions are allowed to impinge (see figure 1). At the zone of impingement, droplets penetrate into the opposite stream due to their inertia and decelerate until stagnation due to the gas drag force. Afterwards, the droplets accelerate and penetrate into the original stream, and so forth. Thus, droplets perform damped oscillations, and the pressure gradient in the gas acts as a restoring force. These droplet oscillations between the streams result in increased droplet residence times. The relative velocity between the droplets and the gas phase in the zone of impingement is significantly increased, which results in an enhancement of convective heat and mass transfer rates between the phases. The above advantages of impinging streams reactors have motivated their employment for various gas–liquid operations, such as the absorption of gases into a dispersed liquid and the combustion of liquid fuels, and the results obtained have indicated a significant increase in interphase transfer rates with respect to reactors of other types (see Elperin 1972; Tamir & Kitron 1987; Herskowits *et al.* 1988). Experimental investigations of fuel combustion in such reactors performed by Elperin (1972) have demonstrated the practically complete combustion of high sulphur-content oil with low levels of sulphur dioxide and soot in combustion products.

Particle collisions apparently decrease particle residence times in the reactor, thereby impairing the reactor performance for solid particle suspensions, as was reported by Elperin (1972),

but possibly enhance mass transfer through droplet breakup, as was observed by Elperin (1972) and Herskowits *et al.* (1988).

Collisions between droplets are caused by differences in droplet velocities. The differences in velocities arise particularly from the interaction of droplets from opposite streams, but may also arise due to differences in response to a flow field by droplets of different size or mass, flow field shear and turbulence, wakes and flow instabilities. When the droplet number density is sufficiently high and/or when there are intrinsic random effects in the flow field of the carrying gas (i.e. turbulence), these collisions can be accounted for with the aid of methods developed in non-equilibrium statistical mechanics.

The evolution of droplet size distribution in spatially homogeneous droplet clouds involving coalescence has been studied extensively [see the review in Pzuppacher & Klett (1978) and Pearson *et al.* (1984)]. Kinetic equations were derived describing the change with time of the droplet size probability density function. The expression for droplet collision rates in these kinetic equations incorporates a collection kernel, which is calculated from the expected droplet relative velocity and the impaction efficiency in collision. Collection kernels have been suggested for Brownian and turbulent coagulation, gravitational sedimentation, thermophoresis and diffusiophoresis. Gillespie (1975) rigorously derived a Monte Carlo procedure for modelling the stochastic coalescence process, employing such collection kernels. Numerous numerical simulations have been performed, yielding results in agreement with experimental observations (e.g. Pzuppacher & Klett 1978; Pearson *et al.* 1984). The kinetic equations and numerical methods for the calculation of droplet size distribution in homogeneous clouds, taking into account the droplet breakup and rebound in collisions, as well as coagulation, were also developed [e.g. Gillespie & List (1979) and the review in Pzuppacher & Klett (1978, Chap. 5)]. Brown (1985) proposed finite-difference schemes for solving a coalescence–breakup equation for rain drops in the atmosphere, where the drops were assigned terminal falling velocities.

Inhomogeneous gas–droplet flows have received considerable attention (e.g. Faeth 1983). Mostafa & Elghobashi (1985) and Mostafa & Mongia (1987) have recently solved a system of coupled conservation equations governing the flow in a turbulent jet laden with vaporizing droplets. They employed a Lagrangian approach to describe droplet motion in a turbulent velocity field and used expressions for droplet turbulent diffusivity in the gas. The equations were solved by a finite-difference technique. In these studies, the suspension was assumed to be sufficiently dilute for droplet collisions to be neglected.

However, only a few studies have considered inhomogeneous flows of droplets undergoing collisions. Tambour (1985a) and Greenberg *et al.* (1986) analysed the droplet size distribution in an evaporating spray with droplet coalescence by the sectional representation method [see also Gelfand *et al.* (1980)]. In this method the droplet size domain is divided into sections and in each section the evolution of only one integral quantity is considered (e.g. number, surface area or volume of droplets in the section). This method correctly predicts the droplet size and spatial distributions in a turbulent fuel spray with vaporization and combustion. O'Rourke (1981) has thoroughly analysed the vaporization of fuel droplets in a turbulent jet, taking into account collisions between droplets, particularly droplet coagulation. The relevant mass, momentum and energy conservation equations were solved numerically. This method treats droplet collisions through a Monte Carlo procedure similar to that applied in the present work, but the collision dynamics model involves many approximations.

The aim of this research is to develop a stochastic model and to provide a Monte Carlo method for modelling the flow of interacting liquid droplets suspended in a rapidly flowing gas stream, and to apply this method to evaluate flow parameters in an impinging streams reactor. The model suggested in this work will focus on the effects of droplet collisions, treating thoroughly the sampling of colliding droplets and the collision dynamics.

2. STOCHASTIC MODEL FOR DROPLET COLLISIONS IN SPRAYS

An analogy between droplet collisions in suspensions and molecular collisions, described in the kinetic theory of gases, enables the application of the Boltzmann equation for droplets, as first suggested by Pai (1974).

Consider the flow of a gas carrying droplets under the following assumptions. For sufficiently small and dense droplets, the droplets may be assumed to be spherical during their collisionless motion. The suspension is considered to be dilute and the collision durations sufficiently short. Then the droplet motion can be described as collisionless motion due to forces exerted by the gas, interrupted by droplet collisions. Therefore the developed model cannot take into account the deviation of the trajectories of colliding particles due to hydrodynamical interaction, causing a reduction in collision rate (e.g. Langmuir & Blodget 1948). Only binary collisions between droplets with uncorrelated pre-collision velocities are considered. These assumptions are similar to those made in the derivation for the Boltzmann kinetic equation in gas dynamics [see, for example, Lifshitz & Pitaevskii (1981, pp. 67–72)].

The interactions observed for colliding water droplets by Ashgriz & Givi (1987) may involve: (1) a bouncing collision; (2) a grazing collision, in which the droplets just touch each other slightly without coalescence; (3) a permanent coalescence; (4) temporary coalescence followed by a separation in which satellite droplets are generated; (5) a shattering collision, occurring at high energy collisions, in which numerous tiny droplets are expelled radially from the periphery of the interacting drops. Since the dynamics of such collisions are very complicated, the available expressions for predicting their outcomes are as yet mostly empirical. The results reported recently by Podvisotsky & Shraiber (1984) have been chosen in this work due to their applicability to a flowing gas–droplet suspension and their capabiity to predict post-collision velocities for fragments. According to these results, a target droplet i colliding with a projectile j (smaller than the target droplet) undergoes a mean change in mass, given as

$$\Delta m_i/m_j = 1 - 0.246\,\mathrm{Re}_{ji}^{0.407}\,\mathrm{Lp}_i^{-0.096}(\delta_i/\delta_j)^{\,0.278} - \phi_{ij}$$

$$(\text{for } 30 < \mathrm{Re}_{ji} < 6000; \quad 5 < \mathrm{Lp}_i < 3.10^5; \quad 1.9 \leqslant \delta_i/\delta_j \leqslant 12), \qquad [1]$$

where m is a droplet mass; Re_{ji} is the Reynolds number for a small droplet penetrating into a larger droplet,

$$\mathrm{Re}_{ji} = \delta_j|\mathbf{v}_j - \mathbf{v}_i|\rho_\mathrm{p}/\mu_\mathrm{p}, \qquad [2]$$

where δ is a droplet diameter, $\mathbf{v}$ is a droplet velocity, ρ_p is its density and μ_p is the liquid particle viscosity; Lp_i is the Laplace number, indicating a ratio between surface tension forces and viscous drag,

$$\mathrm{Lp}_i = \delta_i\rho_\mathrm{p}\sigma_\mathrm{p}/\mu_\mathrm{p}^2, \qquad [3]$$

where σ_p is the surface tension between the droplet and the gas; ϕ_{ij} is a correction term accounting for the gas flow, given as

$$\phi_{ij} = \begin{cases} 0.00446 \cdot A & \text{for } A \leqslant 40.6 \\ 11.85 \cdot (0.01A)^{4.64} & \text{for } 40.6 \leqslant A \leqslant 120, \end{cases} \qquad [4]$$

$$A = \mathrm{Re}_{ji}^{0.285}\,\mathrm{Lp}_i^{0.2}(\delta_i/\delta_j)^{0.4}\mathrm{We}_i^{0.442}; \qquad [5]$$

and We_i is the Weber number, indicating a ratio between the inertia force and the surface tension force,

$$\mathrm{We} = \rho_\mathrm{g}|\mathbf{U} - \mathbf{v}|^2\delta/\sigma, \qquad [6]$$

where $\mathbf{U}$ is the local gas velocity. When $m_i/m_j = 1$, the droplets coalesce. When $0 < \Delta m_i/m_j < 1$, some of the projectile droplet is fragmented. For $-m_i/m_j < \Delta m_i/m_j < 0$ (the condition $-m_i/m_j < \Delta m_i/m_j$ is imposed by conservation of mass), the projectile droplet is fully fragmented while the target droplet is fragmented partially or fully. From [1] it is evident that the probability for coalescence increases when the ratio between diameters of target and projectile droplets approaches one (for zero relative velocity between the target droplet and the gas). This dependence fits the findings of McTaggart-Cowan & List (1973), who reported that excessively small projectile droplets failed to coalesce. The likelihood of droplet fragmentation increases for higher values of relative velocities of colliding droplets and gas–droplet slip velocity. Fragmentation is also facilitated when the surface tension and gas drag are small relative to inertial forces. The above features of [1] fit expressions developed for estimating limits between coalescence and fragmentation

modes in collisions [as in the widely cited work of Brazier-Smith *et al.* (1972)], although it has been found experimentally by Podvisotsky & Shraiber (1984) that such expressions are often unreliable. Notably, according to [1], the gas flow may considerably enhance droplet fragmentation by collisions; this effect was not accounted for in expressions used in earlier works. Since no information is available about the distribution of the mass change $\Delta m_i/m_j$, the mean value given by [1] is used in this work as a single value.

The distribution of diameters for the fragments formed in a collision (excluding the larger droplet, the diameter of which is determined by [1]) has been correlated by Podvisotsky & Shraiber (1984) as a log-normal distribution of the reduced variable $\bar{\delta}_k = \delta_k/\delta_i$ (δ_k = fragment diameter).

$$P[\bar{\delta}_k] = [(2\pi)^{1/2}\bar{\delta}_k\sigma_d]^{-1}\exp[-(\ln\delta_k - \ln\epsilon_d)2\sigma_d^2], \quad [7]$$

where parameters ϵ_d and σ_d are given by

$$\ln\epsilon_d = -1.13\,We_i^{0.08}Re_{ji}^{0.65}Lp_i^{-0.57}(\delta_i/\delta_j)^{0.25} \quad [8]$$

and

$$\sigma_d = 0.61We_i^{-0.15}Re_{ji}^{0.11}Lp_i^{0.014}(\delta_i/\delta_j)^{-0.16}. \quad [9]$$

In the above distribution the predicted mean fragment diameter decreases and the scatter in sizes increases as the effect of inertia forces exceeds that of surface tension and gas drag. The above size distribution is in qualitative agreement with the data presented by Bradley & Stow (1979).

The following correlation has been developed by Podvisotsky & Shraiber (1984) for the velocity of fragments scattered following the collision:

$$(\mathbf{v}_k - \mathbf{v}_i)\cdot(\mathbf{v}_j - \mathbf{v}_i)/|\mathbf{v}_j - \mathbf{v}_i|^2 = 0.08 + 0.016We_i = \beta_v \quad \text{for } We_i \leqslant 12.5, \quad [10]$$

where $\mathbf{v}_k$ is the velocity of fragment k. This expression indicates that the fragment velocity (in a frame moving with the target droplet initial velocity) may be smaller by an order of magnitude than that of the projectile droplet, and that this velocity increases with the Weber number. The latter may be expected, for when the ratio between inertia forces and surface tension is high, the fragments retain considerable amount of initial kinetic energy following the collision. In addition to the above empirical correlation, conservation of momentum must hold:

$$m_i\mathbf{v}_i + m_j\mathbf{v}_j = (m_i + \Delta m_i)\mathbf{v}_i' + \sum_{k=1}^{v} m_k\mathbf{v}_k, \quad [11]$$

where $\mathbf{v}_i'$ is the post-collision velocity of the target droplet i and v is the number of fragments formed. When the droplets do not coalesce, [10] and [11] do not suffice for calculating the fragments velocities. Hence, in this work it is assumed that the fragment direction of motion is isotropic in a frame moving with the colliding droplets center-of-mass velocity ($\mathbf{v}_{c.m.}$). Given a unit vector $\mathbf{x}$ in this direction, [10] yields:

$$\beta_v = [v_k'\cdot\mathbf{x} + \mathbf{v}_{c.m.} - \mathbf{v}_i]\cdot[\mathbf{v}_j - \mathbf{v}_i]/|\mathbf{v}_j - \mathbf{v}_i|^2 = \{[v_k'\cdot\mathbf{x}\cdot(\mathbf{v}_j - \mathbf{v}_i)] + (\mathbf{v}_{c.m.} - \mathbf{v}_i)(\mathbf{v}_j - \mathbf{v}_i)/|\mathbf{v}_j - \mathbf{v}_i|^2, \quad [12]$$

where v_k' is the fragment speed, in a frame moving with the colliding droplets center-of-mass velocity. The fragment velocity in the laboratory frame is thereby determined as

$$\mathbf{v}_k' = \mathbf{x}[\beta_v|\mathbf{v}_j - \mathbf{v}_i|^2 - (\mathbf{v}_{c.m.} - \mathbf{v}_i)(\mathbf{v}_j - \mathbf{v}_i)]/[\mathbf{x}\cdot(\mathbf{v}_j - \mathbf{v}_i)] + \mathbf{v}_{c.m.}. \quad [13]$$

Once the fragment velocities have been calculated, the target droplet post-collision velocity may be determined from the conservation of momentum ([11]). This calculation method must be constrained by the conservation of energy, so that the sum of kinetic and surface tension energies following the collision does not exceed the value of that sum prior to the collision:

$$m_iv_i^2/2 + m_jv_j^2/2 + \sigma_p\pi(\delta_i^2 + \delta_j^2) \geqslant (m_i + \Delta m_i)v_j'^2 + \sigma_p\pi(\delta_j')^2 + \sum_{k=1}^{v}(m_kv_k^2 + \sigma_p\pi\delta_k^2), \quad [14]$$

where δ_i' is the target droplet post-collision diameter, calculated from its new mass $m_i + \Delta m_i$. If the latter condition does not hold, new post-collision fragment directions must be sampled and if repeated samplings do not suffice, fragment sizes are resampled. It is assumed that droplet

atomization by the gas shear during free motion can be neglected. However, a change of droplet size due to vaporization is taken into account.

Applying this collision dynamics model and the assumptions listed above, the Boltzmann equation for the droplet distribution function $f(\mathbf{r}, \mathbf{v}, \delta, t)$ may be derived following the approach used in molecular gas dynamics (e.g. Lifshitz & Pitaevskii 1981, pp. 7–11). This procedure is similar to the derivation of kinetic equations for solid particle distributions in gaseous suspensions (e.g. Kitron *et al.* 1990). Since the obtained non-linear integro-differential kinetic equation is as yet beyond analytical solution, numerical methods must be employed. Although Monte Carlo methods have been extensively used to solve various rarefied gas dynamics problems, only a few attempts have been made to apply these methods to suspension flows. Recently, a Monte Carlo simulation method for calculation of the solid particle distributions in impinging streams reactors has been developed by Kitron *et al.* (1990). In this work a Monte Carlo simulation procedure is derived for solving the kinetic equation for the droplet distribution function, taking into consideration gas–droplet interaction effects, inhomogeneity of the flow field and binary droplet collisions, resulting in either coagulation or fragmentation of colliding droplets.

3. EMPLOYMENT OF THE MONTE CARLO DIRECT SIMULATION METHOD

In this work, the direct simulation Monte Carlo (DSMC) method, first suggested by Bird (1976) for solving the Boltzmann equation in molecular gas dynamics, is used for modelling droplet interactions in dense fuel sprays. The key ideas of the DSMC method are: (a) the uncoupling of molecular motions and collisions during a time step Δt_m, i.e. the use of the operator-splitting technique; (b) the simulation of molecular collisions by disregarding molecular position coordinates within spatial cells; and (c) the simulation of fewer particles than those in the real flow, while normalizing the collision cross-section so that the collisions rate is not changed. Assumption (a) is valid when Δt_m is smaller than the time between collisions and larger than the collision duration, and assumption (b) is valid provided that the cell is so small that the spatial variation of flow variables in the cell is negligible. Assumption (c) may not be necessary for solid suspension flow, due to relatively small particle number densities; in this work, however, the large number of fragments formed requires that this procedure be implemented.

Under the assumptions listed above the DSMC method for the solution of the Boltzmann kinetic equation describing the flow of a gas–droplets suspension can be formulated as follows. The flow system is divided into equal-volume cells. Simulated droplets are distributed in the system, with their positions, sizes and velocities sampled from the initial distribution function. When a stationary kinetic equation is solved, the initial distribution function is chosen arbitrarily, and the stationary solution is obtained by relaxation techniques for long process times. The droplet population is normalized such that each k_f droplets of identical size in the real system is substituted by one droplet in the simulation, having the same diameter as these droplets. The collision cross-section for each such simulated droplet is accordingly increased by the factor k_f so as to preserve the true collision rate. Provided that the droplet distribution function at time $(n-1)\Delta t_m$ is determined, the distribution function at time $n\Delta t_m$ is calculated as follows. Droplets are allowed to move in the system, without colliding with each other, for a time interval Δt_m, with each droplet's subsequent position, velocity, temperature and diameter determined from the droplet equation of motion and heat transfer to the gas. Within the time interval Δt_m, a droplet may encounter a boundary: either an open boundary, through which it leaves the system; or a wall, onto which it sticks.

Following the collisionless flow, droplets are allowed to collide with each other. The droplet population is discretized by location and size such that the number of droplets of type k in cell m, having a volume V_m, $N_{m,k}$, is given as

$$N_{m,k}(t) = \int_{V_m} d\mathbf{r} \int_0^\infty d\mathbf{v} \int_{\delta_k^s}^{\delta_k^l} d\delta f(\mathbf{r}, \mathbf{v}, \delta, t), \qquad [15]$$

where δ_k^s and δ_k^l are the lower and upper diameter limits, respectively, for droplets of type k. The total number of droplets in cell m is

$$N_m = \sum_{k=1}^{s} N_{m,k}. \qquad [16]$$

A pair of colliding droplets of types i and j is sampled from the possible pairs of these types with probability $\sigma_{ij}v_{ij}/(\sigma_{ij}^{*}v_{ij}^{*})$, where v_{ij} is the absolute value of relative velocity between the droplets, $\sigma_{ij}=\pi(\delta_i+\delta_j)^2/4$ is the total collision cross-section and v_{ij}^{*} and σ_{ij}^{*} are the maxima of the absolute values of the relative velocity and collision cross-section, respectively, between droplets of type i and j in the cell. To determine the collision outcome, the collision dynamics model defined by [1]–[4] is employed. Some of these expressions were correlated from data obtained for a range of conditions specified above. However, for a complex flow it is difficult to preclude obtaining parameter values beyond those specified (e.g. for heavy droplets formed by coagulation); hence, [1] will be extrapolated in predicting collision outcomes, except for cases in which $\mathrm{Re}_{ji}<30$, $\delta_i/\delta_j>12$ or $\mathrm{Lp}_i>3\times10^5$, for which the coagulation probability is higher and thus complete coagulation will be assumed. For the colliding pair, the target droplet (i) is the larger droplet, and its mass change $\Delta m_i/m_j$ is calculated from [1]. If $\Delta m_i/m_j=1$, coagulation occurs, in which case the mass of the projectile droplet is added to that of the target droplet and the target droplet is removed from the array of simulated droplets. The velocity of the resulting droplet is calculated from the equation of momentum conservation ([11], with $v=0$).

If $-m_i/m_j<\Delta m_i/m_j<1$, fragments are formed by the collision, the sizes of which are sampled from the log-normal distribution [7], from a total mass of Δm_i+m_j (with the projectile droplet removed from the droplet array). Δm_i+m_j serves a maximal value in the sampling of the first fragment mass, and for each additional fragment the maximal value is the residual mass. In order to avoid excessive loading of the calculation with minute fragments, which are likely to be swiftly removed from the reactor, fragments smaller than a certain minimal size will be removed from the reactor upon their formation (or after having diminished, due to evaporation, to such a size). Also, a limitation on the number of fragments formed is imposed by the conservation of energy condition [14]; when this condition is violated, repeated sampling of fragment sizes is performed. Once the sizes of the fragments formed have been determined, for each fragment the direction vector $\mathbf{x}$ is sampled from a uniform distribution on a unit sphere, and from it the fragment velocities are determined from [13]. Following the calculation of the fragment velocities, the target droplet post-collision velocity is calculated from the momentum conservation equation [11]. Finally, the energy conservation condition [14] is checked; if violated, new direction vectors are sampled for the fragments and new velocities are calculated. In a case when $\Delta m_i/m_j=m_i/m_j$, the entire target droplet mass is fragmented. Then fragment sizes are sampled as described above, while in the calculation of velocities one of the fragments is substituted for the target droplet in the energy conservation equation.

After each collision, a time increment

$$\Delta t_{ij}=2\delta_{ij}V_{\mathrm{m}}/[N_{\mathrm{m},i}N_{\mathrm{m},j}k_f v_{ij}\sigma_{ij}], \qquad [17]$$

where $\delta_{ij}=1$ if $i=j$ and $\delta_{ij}=0.5$ otherwise, is added to a time counter T_{ij}^{m} for the collisions between droplets of types i and j (T_{ij}^{m} is used for both i,j and j,i collisions), in cell m. The combination of droplet types having the smallest value of the local time counter T_{ij}^{m} is chosen for the next collision (see Bird 1976, pp. 168–171); if all T_{ij}^{m} values are zero, the combination is randomly sampled. This procedure is repeated until all T_{ij}^{m} values exceed the value $n\Delta t_{\mathrm{m}}$. When the collision density is low, the above procedure overestimates the collision rate. In order to avoid this, the last collision for each combination (i,j) in every cell is accepted as a true collision only with probability $P_{\mathrm{last}}=1-(T_{ij}^{\mathrm{m}}-n\Delta t_{\mathrm{m}})/(\Delta t_{ij,\mathrm{last}})$, where T_{ij}^{m} is the value of the time counter after the last collision increment, $\Delta t_{ij,\mathrm{last}}$, has been added to it. Accordingly, with probability $1-p_{\mathrm{last}}$ the last collision is not taken into account, i.e. the parameters of the droplets involved in the last collisions remain unchanged. The expected number of collisions in cell m during a time interval Δt_{m} between droplets of types i and j is given as

$$M_{ij}^{\mathrm{m}}=N_{\mathrm{m},i}N_{\mathrm{m},j}k_f v_{ij}\Delta t_{\mathrm{m}}\sigma_{ij}/(2\delta_{ij}V_{\mathrm{m}}), \qquad [18]$$

where v_{ij} is the mean of the absolute value of relative velocity between droplets of classes i and j. The performance of the procedure depends upon the choice of cell dimensions and the value of the time increment Δt_{m}. The detailed description of the procedure for determination of these parameters is presented in Kitron *et al.* (1990). The same procedure was adopted in the present study.

4. DROPLET EQUATION OF FREE MOTION AND LIMITATIONS ON SUSPENSION PROPERTIES

In the study by Kitron *et al.* (1990), it was shown that the particle volume fraction in a gas–solids suspension must be < 0.055 if the binary collisions assumption is to be valid, and that, on the other hand, the minimal volume fraction is such that particle number densities are high enough to allow statistical treatment; the situation in droplet suspensions is similar. Using the approach applied in the latter study, it can be shown that in the systems treated in this work the deviations in approaching droplet trajectories due to gas flow may be neglected; this has also been confirmed experimentally in the case of droplet collisions in rain clouds reported by McTaggart-Cowan & List (1973).

In the above stochastic model, it has been assumed that collision durations are negligible, so that droplet motion can be described as free motion disrupted instantaneously by collisions. This assumption may be valid for solid particles, but is more problematic for droplets and its validity is difficult to assess due to lack of relevant data. Nevertheless, for high collision velocities characteristic for impinging streams reactors, shorter collision durations may be expected.

Another assumption made was that droplets are spherical and that aerodynamic breakup due to gas shear during free droplet motion is negligible. Borisov *et al.* (1981) investigated experimentally the breakup of single droplets moving in a gas flow. Their results show, as in previous works, that droplet breakup does not occur when $We < 6$, and in some conditions at even higher Weber numbers. For characteristic flow parameters in an impinging streams absorber ($\delta = 40\,\mu$m, $\sigma_p = 0.072$ kg/s^2, $|\mathbf{U} - \mathbf{v}| = 40$ m/s, $\rho_p = 1.77$ kg/m^3), a value of $We = 1.6$ is obtained.

A certain restriction may arise concerning the relation between the hydrodynamical relaxation time, given by Stokes law as

$$\tau_h = \rho_p \delta^2/(18\,\mu_g) \qquad [19]$$

and the mean time between collisions. The assumption that colliding particles have uncorrelated velocities is valid in gas dynamics due to the high rate of collisions between molecules (in addition to the high molecule number densities). Since suspension flow involves a much smaller droplet collision rate than molecule collision rates in gas flow, the hydrodynamical damping of post-collision velocities should be strong enough to prevent such a correlation. If hydrodynamical relaxation occurs too quickly, droplets have small slip velocities relative to the gas, so that their velocities are highly correlated with respect to the gas velocity at the location of the collision. The latter conclusion is equivalent to the requirement that the droplet self-collision Knudsen number, estimated from kinetic theory as $Kn = \xi/D = \delta/(2^{1/2}6\beta D)$, where D is a characteristic macroscopic length, ξ is the free path and β is the droplet mean volume fraction, must not considerably exceed the Knudsen number for collisions of droplets with gas molecules, $S = \tau_h U/D$, where U is a characteristic flow velocity. For the characteristic conditions during pentane combustion considered in this work ($\delta = 35\,\mu$m, $\mu_g = 3.05 \times 10^{-5}$ kg m/s, $U_0 = 11.6$ m/s, $\rho_p = 630$ kg/m^3, $\beta = 0.007$, $D = 0.3$ m), one obtains $Kn = 0.002$ and $S = 0.054$, indicating that the effects of both gas drag and droplet collisions are significant. The restrictions on cell dimensions and the values of the time interval Δt_m have been discussed comprehensively by Kitron *et al.* (1990) and the same treatment applies here.

When only fluid drag acts upon droplets during Δt_m, a droplet trajectory is calculated by integrating the ordinary differential equation

$$d^2\mathbf{r}/dt^2 = 0.75\,C_D[\rho_g/(\rho_p\delta)]|\mathbf{U} - \mathbf{v}|(\mathbf{U} - \mathbf{v}) + \mathbf{g}, \qquad [20]$$

where $\mathbf{U}$ is the gas velocity at $\mathbf{r}$, $\mathbf{g}$ is the gravity acceleration and C_D is the gas drag coefficient for a liquid droplet flowing in a gas, given by Hetsroni (1982, Chap. 1, p. 210) as

$$C_D = \begin{cases} 8(3\Theta + 2)/[Re_p(\Theta + 1)] & \text{for } Re_p < 2 \\ \{14.9/Re_p^{0.78} + \Theta[(24/Re_p) + (4/Re_p^{1/5})]\}/(\Theta + 1) & \text{for } 2 < Re_p < 500, \end{cases} \qquad [21]$$

where

$$Re_p = \rho_g \delta |\mathbf{U} - \mathbf{v}|\mu_g \qquad [22]$$

and

$$\Theta = \mu_p/\mu_g. \quad [23]$$

The lift forces acting on the particles due to gas shear (Magnus force, Saffman force etc.) are neglected, since, for droplets in impinging jets, the drag in the direction of the lift force is usually much stronger than the lift force [see also Soo (1969) and Lee & Wiesler (1987)]. The effect of the droplet flow on the flow pattern of the carrying gas is also neglected. This dynamical uncoupling is justified for laminar flows if the particle volume fraction in the system is sufficiently small so that the gas flow is not affected significantly. The ratio of the stress exerted on the gas by droplets to the total pressure gradient in the impinging jets reactor was estimated to be < 0.01. Thus, the momentum decoupling assumptions also holds for the impinging jets flow pattern.

5. GAS FLOW PATTERN IN AN IMPINGING JETS REACTOR

Elperin (1972) has demonstrated that the gas flow pattern in the inter-nozzles region of impinging streams reactors fits the expressions obtained from a potential flow analysis of a gas jet colliding with a wall:

$$U_z = zU_0/H \quad [24]$$

and

$$U_r = rU_0/(2H), \quad [25]$$

where H is the distance from the jet entrance point to the wall (see figure 1), U_z and U_r are the axial and radial gas velocity components, respectively, and U_0 is the initial jet uniform axial velocity. Thus velocity distribution is not valid at the exit from the feed pipes; as an approximation, a discontinuous gas velocity profile was applied, with [24] and [25] used in the inter-nozzle region (for $|z| < H$ and $r < D_2/2$—see figure 1), and $U_z = -zU_0/|z|$ and $U_r = 0$ for all $|z| > H$ and $r < D_2/2$, where D_2 is the inlet nozzle diameter.

In order to analyse the effect of turbulence in the impinging streams reactor, a coarse modification of [24] and [25] above is considered:

$$U_z = -zU_0/H + u_z' \quad [26]$$

and

$$U_r = rU_0/(2H) + u_r', \quad [27]$$

where u_z' and u_r' are the axial and radial turbulent velocity components, respectively. u_z' and u_r' are assumed to be random Gaussian fields with zero means and with standard deviations chosen as characteristic values from experimental data on turbulent jets impinging upon walls performed by Donaldson *et al.* (1971): $(\bar{u}_z'^2)^{1/2} = 0.01\ U_0$ and $(\bar{u}_r'^2)^{1/2} = 0.15\ U_0$.

Turbulent velocity pulsations are assumed constant during the average lifetime of a turbulent eddy, estimated as the Lagrangian time scale of the turbulent gas flow (e.g. Kitron *et al.* 1990):

$$\tau_\lambda = \Lambda_g/[(\bar{u}_r')^2 + (\bar{u}_z')^2]^{1/2}, \quad [28]$$

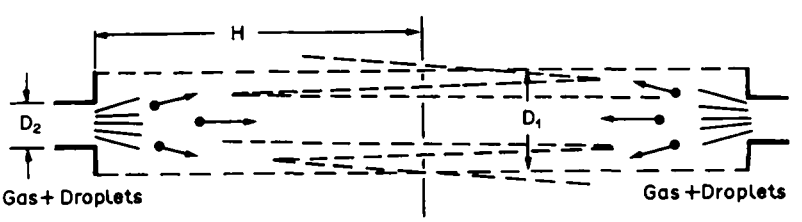

Figure 1. Scheme of an impinging streams reactor for gas–liquid droplet operations.

where τ_i is the average time required for fresh fluid to surround a large particle, or an average time for a very small particle to travel the minimal characteristic length of the turbulent velocity field, and the Lagrangian spatial integral scale Λ_g may be estimated according to Melville & Bray (1979):

$$\Lambda_g = 0.195\, w_{1/2}, \qquad [29]$$

where $w_{1/2}$ is the jet half-width. The above approach requires that the particles be unaffected by the motion of the smallest eddies. This requirement is violated when the hydrodynamical relaxation time τ_h is of the same order of magnitude as the characteristic time for the motion of the smallest eddies, $\tau_s = [\mu_g/(\rho_g \epsilon_t)]^{1/2}$, where ϵ_t is the specific energy dissipation rate. Then, using [19] for τ_h, the restriction on the droplet diameter is

$$\delta \sim L_K/(18\rho_p/\rho_g)^{1/2}, \qquad [30]$$

where L_K is the Kolmogorov microscale length,

$$L_K = [\mu_g^3/(\rho_g^3 \epsilon_t)]^{1/4}. \qquad [31]$$

Therefore, for large values of $\rho_p/\rho_g \sim 1000$, as studied in this work, only droplets smaller by 2 orders of magnitude than the Kolmogorov microscale length may respond to the smallest eddies. For air flow with a characteristic value of $\epsilon_t = 300$ W/kg: $L_K \sim 0.06$ mm, so that the above restriction is violated only for submicronic droplets. For comparison, let us calculate the Lagrangian scale for characteristic flow values of $(\bar{u}'^2)^{1/2} = 2$ m/s and $\epsilon_t = 300$ W/kg, obtaining $\Lambda_g = \tau_i(\mu'^2)^{1/2} = 3$ mm, which is larger by 1–2 orders of magnitude than the diameters of droplets studied in this work. As mentioned above, the modulation of the gas turbulence pattern caused by droplets is neglected. The latter approximation was validated in Kitron *et al.* (1990) by numerical sensitivity studies, in which numerical simulation results were only weakly affected by changing the Lagrangian time scale by a factor of ~ 2.

In the simulation, droplet motion inside an impinging streams reactor will only be calculated in the range $0 < z < H$, so that the reactor symmetry with respect to the impingement plane may be exploited. The impingement plane will be treated as a specularly reflecting surface and droplets will be assumed to leave the reactor upon crossing a certain maximal radius measured from the reactor axis. Following each time interval Δt_m, a droplet mass of $F_L \Delta t_m$, where F_L is the liquid mass feed rate, is fed to the reactor inlet. The diameters of droplets within this mass are sampled from a log-normal distribution with parameters determined from experimental data; the log-normal distribution is applied since it closely describes the features of the size spectrum obtained from spray nozzles. The droplet inlet velocity is assumed to be uniform and equal to the gas inlet velocity, U_0, estimated as $4F_G/(\rho_g \pi D_2^2)$, where F_G is the gas inlet mass flow rate. The initial droplet volume fraction, β_0, used to calculate Δt_m, is determined as $\beta_0 = F_L \rho_g/[\rho_p F_G]$. Droplets are fed at radial positions sampled from the uniform distribution over the inlet nozzle cross-section. In order to simulate a continuous droplet feed, an initial axial position of each droplet is calculated by integration of the equation of motion [20] during a random fraction of Δt_m, with initial conditions $v = U_0$ and $z = H$.

6. CALCULATION OF GAS ABSORPTION IN IMPINGING STREAMS ABSORBERS

Herskowits *et al.* (1988) have investigated the performance of an impinging streams reactor for gas absorption in a liquid phase. The reactor consisted of two oppositely positioned spray nozzles, which released two impinging water spray jets into a chamber containing CO_2. The quantity of CO_2 absorbed in the water was measured for different operating conditions. To evaluate the performance of this reactor, assume that the system is isothermal and that the dominant resistance to mass transfer is inside the thin spherical shell within a liquid droplet, within radii $r_1 < r < r_2$. Neglecting the gas phase resistance may be justified for the absorption or desorption of a pure gas with low solubility by a weakly volatile liquid. In the latter case, the diffusivity coefficient for the gas in the gaseous phase is much greater than in the liquid phase, and its concentration in a gaseous phase in equilibrium with the liquid phase is close to its concentration in the bulk gaseous phase.

Therefore, the gas concentration gradient in the gaseous phase is small, so that the gas phase resistance may be neglected. On the other hand, a characteristic time for mass transfer inside the droplet is

$$\tau_D = \delta^2/D_{gL}, \quad [32]$$

where D_{gL} is the diffusivity of the gas in the liquid, which for CO_2 in water is 1.9×10^{-9} m^2/s (see Perry & Chilton 1973, Chap. 3, p. 224). For a 40 μm dia droplet, $\tau_D = 0.85$ s compared with about 10^{-6} s for the hydrodynamical relaxation time and with a residence time in the reactor of at least 0.01 s (estimated as L/U_0). Thus, it is evident that the rate of mass transfer process within the droplet determines the total mass transfer rate. The validity of neglecting the gas phase resistance on the mass transfer in this system was also confirmed by experimental results reported in Tamir & Kitron (1987), whereby the gas flow rate in an impinging streams absorber with separate gas and liquid inlets had an insignificant effect on the absorption rate.

Then, under the above assumptions and following Brid *et al.*'s (1960, p. 528) analysis, the rate of mass transfer of a component A from the gas to the liquid droplet is determined as follows:

$$T_A = \{4\pi c D_{AL}/[(1/r_1) - (1/r_2)]\}\ln[(1 - x_{A2})/(1 - x_{A1})], \quad [33]$$

where c is the overall molar concentration in the liquid droplet, D_{AL} is the diffusivity of component A in the liquid phase, and x_{A1} and x_{A2} are the molar fractions of component A at radii r_1 and r_2, respectively. Assuming that $r_2 = \delta$ and $r_1 - r_2 = \eta$, where $\eta \ll \delta$, and assuming that the droplet is in a quasi-steady state so that the changes in η, x_{A1} are negligible, [33] reduces to:

$$T_A = (4\pi c\delta^2 D_{AL}/\eta) \cdot \ln[(1 - x_{A2})/(1 - x_{A1})] = k_L(4\pi\delta^2 D_{AL})\ln[(1 - x_{A2})/(1 - x_{A1})], \quad [34]$$

where k_L is the mass transfer coefficient which may be treated as constant and $4\pi\delta^2 = A$ is the contact area between the phases. Then, an evaluation of the transfer rate may be obtained by calculating the time-averaged interphase area in a steady-state flow:

$$\bar{A} = \left(\int_{t_1}^{t_2} A \, dt'\right)\Big/(t_2 - t_1). \quad [35]$$

7. EVALUATION OF FUEL VAPORIZATION AND SPRAY COMBUSTION

The combustion of liquid fuel spray in a combustion chamber is commonly encountered in furnaces, gas turbines, diesel engines etc. In such processes, a dominant rate controlling factor is the rate of fuel vaporization from the spray droplets, since the combustion occurs in the gaseous phase. Extensive efforts have been devoted to the modelling of fuel vaporization in spray combustion (e.g. Faeth 1983; Sirignano 1983). The results obtained by Tambour (1985a) indicated that coalescence significantly affected the droplet size distribution in the spray center, whereas close to the spray edges the effect of vaporization was more dominant.

In order to evaluate the effect of droplet collisions on liquid fuel combustion in an impinging streams reactor, the results of Faeth's (1983) analysis of single drop behaviour in fuel sprays were employed. The Faeth expression for droplet vaporization rate is valid for a moving droplet when the gas phase Damkohler number,

$$\mathrm{Da} = \delta/(\tau_r|\mathbf{v} - \mathbf{U}|), \quad [36]$$

where τ_r is a characteristic reaction time, is small and when the reaction is confined to the bulk gaseous phase. A local homogeneous flow analysis performed by Faeth (1983) has yielded small values of the Damkohler number, indicating that the assumption is reasonable. Moreover, experimental data discussed by Faeth (1983) revealed appreciable quantities of unburned gaseous fuel within the core of well-attached spray diffusion flames, indicating that most drops simply evaporated with no envelope flames present.

Following Faeth's (1983) analysis, the vaporization rate from each droplet is given as

$$\dot{m} = 2\pi\delta\rho_d D_F \cdot \ln[(1 - Y_F)/(1 - Y_{Fsg})] \cdot \{1 + 0.278\,\mathrm{Re}^{1/2}\mathrm{Sc}^{1/3}/[1 + 1.232/(\mathrm{ReSc}^{4/3})]^{1/2}\}, \quad [37]$$

where $\dot{m}$ is the mass vaporization rate, D_F is the diffusion coefficient for the vaporized fuel in the gaseous phase, Y_F is the fuel vapour fraction in the gaseous phase, Y_{Fsg} is the fuel vapour fraction in the gas–liquid interface and Sc is the Schmidt number, $Sc = \mu_g/\rho_g D_F$. The equation of conservation of energy for the drop yields:

$$(\pi\rho_p C_p \delta^3/6)(dT_p/dt) = \pi\delta^2 h(T - T_p) - \dot{m}\Delta H, \quad [38]$$

where C_p and T_p are the liquid fuel heat capacity and temperature, ΔH is the enthalpy per mass required to transform the liquid fuel to fuel vapour in the bulk gas temperature and h is the heat transfer coefficient determined as follows:

$$h = [\dot{m}C_p/(\pi\delta^2)]\{1 + 0.278\,Re^{1/2}Pr^{1/3}[1 + 1.232/(RePr^{4/3})]^{1/2}\}/\{\exp[\dot{m}C_p/(2\pi\delta\lambda_g)] - 1\}, \quad [39]$$

where λ_g is the gas thermal conductivity and Pr is the Prandtl number, $Pr = C_{p,g}\mu_g/\lambda_g$. The mixing rule used for determining the viscosity of the gaseous mixture in the reactor is Wilke's semiempirical formula (e.g. Bird *et al.* 1960, p. 34) and a similar mixing rule is used for estimating the thermal conductivity (e.g. Bird *et al.* 1960, p. 258); other mixture properties are calculated by assuming an ideal mixture.

8. VALIDATION OF THE NUMERICAL METHOD

In order to investigate the capability of the above described Monte Carlo simulation procedure to correctly predict droplet size and spatial distributions in spray with droplet interactions, the analysis of flow systems was performed for which results are known in the literature: droplet coagulation and fragmentation in homogeneous and inhomogeneous gas–droplet suspensions.

8.1. Evolution of the droplet size distribution in homogeneous coagulation

Staffman & Turner (1956) have investigated theoretically the formation of a droplet size distribution in a homogeneous rain cloud. The following expression for the collision rate between droplets of types i and j, having diameters δ_i and δ_j, respectively, flowing in a turbulent gas was derived:

$$R_{col} = 1.3(\delta_i + \delta_j)^3 n_i n_j (\epsilon_t \rho_g/\mu_g)^{1/2}/[8(1 + \delta_{ij})], \quad [40]$$

where ϵ_t is the energy dissipation rate in the gas and n indicates number density. Assuming that the rain cloud is spatially homogeneous and that all droplet collisions result in coalescence, Saffman & Turner (1956) calculated the droplet size distributions for different times starting with a population with uniform droplet diameter δ_0. In their calculation, droplet number density was normalized by the initial number density n_0, and time was normalized as follows:

$$\bar{t} = 1.3\,\delta_0^3 n_0 (\epsilon_t \rho_g/\mu_g)^{1/2} t/8 \doteq \alpha_0 t. \quad [41]$$

To analyse this problem using the DSMC method, droplet free motion does not need to be considered, since the collision rate is independent of their positions or velocities. Instead of [18] above, the expected number of i,j collisions in a system of volume V_m during a time interval Δt_m is given by

$$\Psi_{ij} = 1.3(\delta + \delta_j)^3 N_i N_j (\epsilon_t \rho_g/\mu_g)^{1/2}\,\Delta t_m/[8(1 + \delta_{ij})] = \alpha_0(\delta_i + \delta_j)^3 N_i N_j \Delta t_m/[n_0 V_m \delta_0^3(1 + \delta_{ij})] \quad [42]$$

so that for an initial number of droplets N_0, the time increment added for an i,j collision is

$$\Delta t_{ij} = [N_0\delta_0^3(1 + \delta_{ij})]/[(\alpha_0(\delta_i + \delta_j)^3 N_i N_j]. \quad [43]$$

The expected rate of i,j collisions for a single droplet is

$$\nu_{i,j} = \Psi_{ij}/[\Delta t_m N_i] = \alpha_0(\delta_j + \delta_i)^3 N_j/[N_0\delta_0^3(1 + \delta_{ij})] \quad [44]$$

and since the value of Δt_m should be shorter than $1/N_i$, its value may be assigned as $1/[N_0\alpha_0]$. A numerical solution obtained for $N_0 = 30{,}000$, is presented in figure 2, for $t = 0.09$ and compared with results reported by Saffman & Turner (1956). As a result of droplet coalescence without fragmentation, the droplet population consists of groups of droplets with masses that are integer multiples of the initial droplet mass. The results obtained by the DSMC method correctly describe

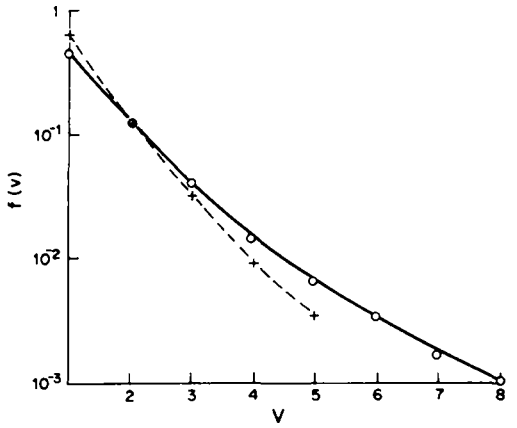

Figure 2. Droplet size distribution in a homogeneous, turbulent rain cloud, for coalescence only and uniform initial sizes distribution; for dimensionless time $t = 0.09$; $N_0 = 30{,}000$. ○, Calculated by Saffman & Turner (1956); +, calculated by the DSMC method.

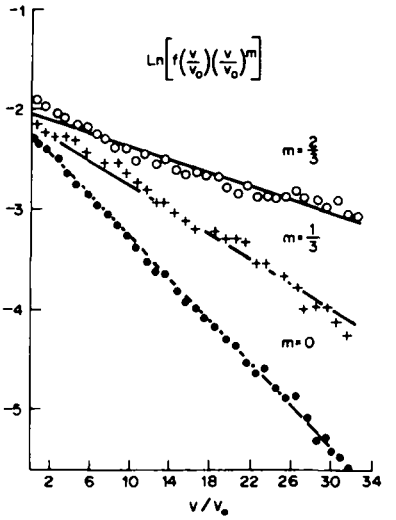

Figure 3. Droplet size distribution calculated in simulation (marked points) compared with the distributions calculated analytically from [47] by substituting (δ^{3m}) values obtained in the simulation (marked lines); V = volume, $V_0 = \pi(0.5\text{ mm})^3/6$. ●, $m = 0$; +, $m = 1/3$; ○, $m = 2/3$.

the solution for droplet populations having concentrations of down to 2% of the initial droplets concentration. For smaller concentrations, corresponding to larger droplet sizes, the Monte Carlo solution underestimates the concentration values. Thus, the developed method copes well with predicting the evolution of the droplet size spectrum, but fails to predict the formation of particularly large droplets with small concentrations. Note that due to the homogeneity of the system, collisions were sampled in a single cell with a very large population. Hence, for inhomogeneous flows, for which the population in a cell may be much smaller, statistical errors may be more significant.

8.2. Evolution of the droplet size distribution in homogeneous coagulation and fragmentation with size-dependent collision cross-section

A second check, intended to examine the simulation method capability to sample collisions while accounting for different collision cross-section and a different collision dynamics model, was performed for a spatially homogeneous system, with the collision rate given as:

$$R_{\text{col},ij} = \alpha N_i N_j (\delta_i^3 \delta_j^3)^m / (1 + \delta_{ij}), \qquad [45]$$

where α is a constant, so that the collision cross-section is proportional to $(\delta_i \cdot \delta_j)^{3m}$. The conditional probability density distribution $g(v_i, v_j, v)$ of secondary droplets volumes v was assumed to have a uniform distribution so that

$$g(v_i, v_j, v) = \begin{cases} 1/(v_i + v_j) & \text{if } -v_i < v < v_j \\ 0 & \text{otherwise,} \end{cases} \qquad [46]$$

where v_i and v_j are the volumes of colliding droplets. For this system, the droplet volumes probability density function at steady state was found analytically by Bajpai *et al.* (1988):

$$f(\delta^3) = \begin{cases} \exp[-\delta^3/\bar{\delta}^3]/(\bar{\delta}^3) & \text{if } m = 0 \\ \xi \exp[-\delta^3/\omega]/\delta^{3m} & \text{otherwise} \end{cases} \qquad [47]$$

with

$$\xi = \bar{\delta}^{3m} / \{[\bar{\delta}^{3m}\, \Gamma(1 - m)]^{1/m}\} \qquad [48]$$

and

$$\omega = [\bar{\delta}^{3m}\, \Gamma(1 - m)]^{1/m}, \qquad [49]$$

where $\bar{\delta}^i$ indicates the ith moment of the droplet diameter distribution function and $\Gamma(\cdot)$ is the gamma function. The above Monte Carlo method was applied to calculate the steady-state size distributions for the cases $m = 0$, $m = 1/3$ and $m = 2/3$. The evolution of the initial population of 10,000 droplets with a log-normal size distribution, $P(\delta) = [(2\pi)^{1/2}\delta\sigma^*]^{-1}\exp[(-(\ln\delta - \mu^*)/2(\sigma^*)^2]$ with $\sigma^* = 0.2$ and $\mu^* = 0.0$, was considered. The droplet population was discretized in the calculation by dividing volumes by the volume of a droplet with $\delta = 0.5$. In figure 3, the obtained size distributions are compared with those predicted analytically by substituting the values of the moments $\bar{\delta}^{3m}$ obtained in the numerical calculation in [47] above. Clearly, a good agreement is obtained, demonstrating the capability of the numerical method to provide correct solutions in the case of size-dependent collision cross-sections.

8.3. Evolution of the droplet size distribution in inhomogeneous coagulation and fragmentation with size-dependent collision cross-section

A third system analysed was that described by Gillespie & List (1979) for a rain cloud, in which size distributions change as a function of the height above ground. They assumed that the problem may be described as one-dimensional (in a direction perpendicular to the ground). Also, stationary flow was considered, with a source supplying rain drops at the cloud top having a Marshall–Palmer (1976) size distribution:

$$p_{\text{source}}(\delta) = \Lambda_0 \exp(-\Lambda_0\delta). \qquad [50]$$

The effects of side winds and condensation and vaporization during droplet fall were neglected. It was also assumed that droplet velocities equalled their free-fall values, estimated by Best's (1950) formula. The same assumptions were made in this study, while applying a collision dynamics model proposed by Brazier–Smith *et al.* (1972), which accounts for both fragmentation and coagulation. According to this model, the probability of droplet coalescence is given as

$$p(\delta_i, \delta_j) = \begin{cases} (1 + \delta_j/\delta_i)^{\ 2} & \text{if } \delta_i > 0.5\,\text{mm} \\ 0 & \text{otherwise.} \end{cases} \qquad [51]$$

If the droplets do not coagulate, the collision outcome is calculated from data reported by McTaggart-Cowan & List (1973), whereby the probability density function of target droplet post-collision mass is given as

$$P_1(m_i'; m_i, m_j) = \begin{cases} \eta \exp[-(m' - m_i)^2/(2s^2)] & \text{if } m' < m_i + m_j \\ 0 & \text{otherwise,} \end{cases} \qquad [52]$$

where the coefficient η is correlated as

$$\eta = 11.8/[\delta_i^4\delta_j(0.41 - 0.3\delta_j/\delta_i)] \qquad [53]$$

and the variance s^2 is recursively determined from the normalization condition [52]. The mean number of fragments formed in the collision is correlated as

$$f = 3.6[(\delta_i^3\delta_j)(0.41 - 0.30\delta_j/\delta_i)]^{1/2} \qquad [54]$$

and the probability density function of the fragment mass is given by

$$p_f(m_f; m_i, m_j) = \begin{cases} (6.0f/\delta_i)(m_f/0.0654)^\alpha/\Phi & \text{if } m_f < 1 \\ (6.0f/\delta_i)m_f^{2.6}/[0.0654)^2\Phi] & \text{otherwise,} \end{cases} \qquad [55]$$

where Φ is a normalization factor obtained by normalizing the above distribution function in the range $(m_{\min}, m_i + m_j - m_i')$; $m_{\min}$ is a minimal fragment mass which was assigned by Gillespie & List (1979) as 0.0654 mg; $\alpha = -1.0 - 0.392/\delta_j$.

The Monte Carlo simulation was applied for a cloud with a cross-section value of 2000 mm^2. For the conditions considered by Gillespie & List (1979), with a rain deposition rate of 25 mm/h, a cloud of height 2 km and a Marshall–Palmer parameter value $\Lambda_0 = 2.09\,\text{mm}^{-1}$ (corresponding to an initial droplet number density of 4×10^{-6} droplets/mm^3), the total number of droplets obtained in the simulation system at steady state was about 36,000. The resulting droplet size distribution, calculated following 500 time intervals of 10 s each and using a normalization factor value of $k_f = 3$, is shown in figure 4 in comparison with that obtained by Gillespie & List (1979).

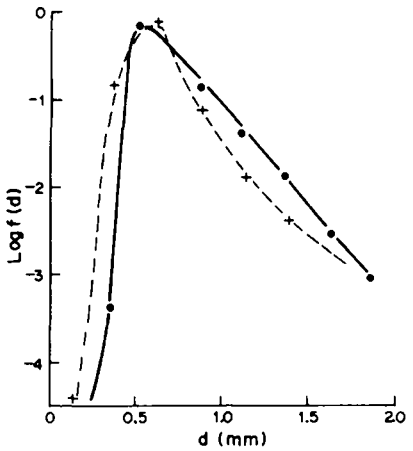

Figure 4. Droplet size distribution in a rain cloud, close to the ground surface ($R = 25$ mm/h, $\Lambda_0 = 2.09\ \text{mm}^{-1}$, cloud height = 2 km). ●, Gillespie & List (1979) solution; +, DSMC solution.

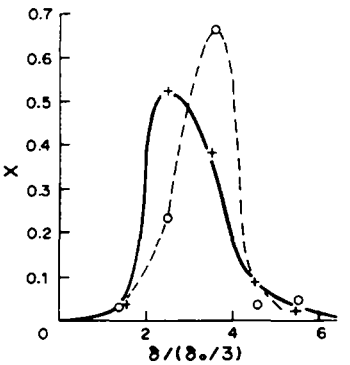

Figure 5. Calculated droplet size distributions in an impinging streams absorber,

$$X = \int_{r_{i-1}}^{r_i} \mathrm{d}\mathbf{r} \int_{\delta_{i-1}}^{\delta_i} \mathrm{d}\delta f(\delta, \mathbf{r}, t) \Big/ \left[\int_{r_{i-1}}^{r_i} \mathrm{d}\mathbf{r} \int_0^{\infty} \mathrm{d}\delta f(\delta, \mathbf{r}, t) \right]$$

($2H = 60$ mm, $k_f = 10$). ——, $z/H = 0.95$; , $z/H = 0.75$.

Clearly, the Monte Carlo solution predicts well concentrations of droplets with number fraction (with respect to the entire population) $> 0.1\%$. The good agreement between the two different solutions demonstrates the capability of the devised Monte Carlo procedure to describe correctly the inhomogeneous dense gas–liquid suspensions with droplet interactions. Notably, coagulation played a major role in obtaining the resulting size distribution, while the role played by fragmentation was practically negligible.

9. NUMERICAL RESULTS AND DISCUSSION

Simulation of spray flows in impinging streams reactors was performed by analysing the reactor shown schematically in figure 1, as described above. The reactor was partitioned in the axial direction (in the range $0 < z < H$) into 10 equal-volume cells.

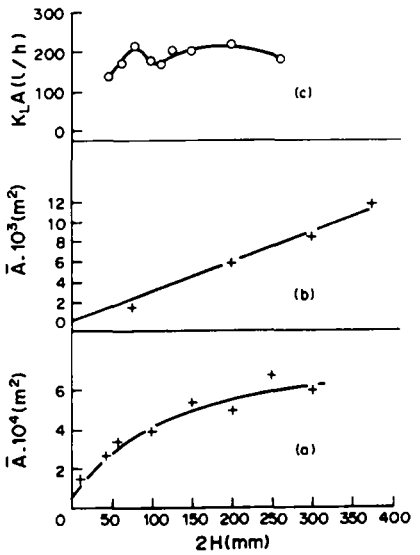

Figure 6. (a, b) Calculated dependence of the average transfer area A on $2H$ for laminar flow in an impinging streams absorber; (a) with collisions, (b) without collision. (c) Experimentally determined (Herskowits *et al.* 1988) dependence of $k_L A$ on $2H$.

9.1. *Numerical analysis of absorption in impinging jets*

The simulation for the absorption process employed parameters relevant to the experimental system used by Herskowits *et al.* (1988): the nozzle diameter was $D_2 = 2$ mm; the gas was CO_2 at atmospheric pressure, fed to each nozzle at a rate $F_G = 4$ kg/h; the liquid was water, fed at $F_L = 40$ kg/h. From these flow rates, the gas inlet velocity was estimated as $U_0 = 207$ m/s and the droplet initial volume fraction as $\beta_0 = 0.018$. Since it was shown in [20] that the reactor efficiency was very weakly dependent on its diameter, the simulation was performed for a minimal reactor diameter, $D_1 = 5$ mm. From experimental data, the droplets fed by the nozzle were known to have a Sauter mean diameter, $\bar{\delta}^3/\bar{\delta}^2$, of 40 μm. By approximating the mean diameter δ as equal to the Sauter mean diameter, and assuming that the standard deviation in δ is 20% of the mean, i.e. $\sigma_\delta = 0.2\bar{\delta}$, the parameters of the log-normal distribution $P(\delta) = [(2\pi)^{1/2} \cdot \delta\sigma^*]^{-1} \cdot \exp[(-(\ln \delta - \mu^*))/2(\sigma^*)^2]$ could be determined from the formulae: $(\sigma^*)^2 = \ln[(\sigma_\delta/\bar{\delta})^2 + 1]$ and $\mu^* = \ln \bar{\delta} - (\sigma^*)^2/2$.

The time increment in the simulation, Δt_m, had a value of 1.8×10^{-6} s, and values of the interphase area A were determined over consecutive periods of 50 Δt_m. When droplet collisions were taken into account, the calculated A values following 5–10 such intervals attained constant values within an accuracy of 5–10%, and steady concentration patterns were assumed. In the absence of such collisions, more droplets accumulated in the reactor and the steady-state condition was attained only following 50–100 such intervals. A typical calculation consumed 400 CPUs on a CDC Cyber 180/860 computer.

The overall steady-state population of droplets in the reactors, when droplets were taken into account, was of the order of 10^5. Hence, the use of a normalization factor k_f was necessary. Values of k_f were in the range 2–10. Changing this factor from 10 to 5 caused an increase in the interphase area by 5–10%; hence, k_f values were chosen as the minimal possible within the calculation capability. In sampling droplet collisions in each cell, the droplet population was discretized by dividing droplet diameters by $\delta_0/3$, where δ_0 indicates the Sauter mean diameter. Droplets with diameter $< \delta_0/4$ were not followed in the calculation.

In collisionless laminar flow in the reactor the droplets concentrated near the reactor plane of symmetry, in accord with the experiments reported by Elperin (1972). This is the result of the known effect of particle accumulation in a region of flow stagnation. Since droplet diameters did not undergo any change in this case, the droplet log-normal size distribution was retained throughout the reactor. When collisions between droplets were taken into account, more droplets were found near the nozzle outlet than near the impingement region. It should be noted that the total concentration for the collisionless flow was larger by a factor of 20 than in the flow with collisions, but in the latter system many droplets were larger, since coagulation exerted a predominant influence. This is seen in figure 5, where droplet size distributions at different axial locations in the reactor are compared; the closer the location is to the impingement plane ($z = 0$), the larger is the fraction of large droplets, formed by coagulation. The fragmentation, on the other hand, was not frequent; calculating the same flow without taking it into account did not change the droplet size distribution significantly.

In figures 6(a, b), the time-averaged overall interphase areas calculated, with and without droplet collisions, for laminar flow, are shown as a function of the nozzle separation distance, $2H$, in the reactor. Collisions between droplets are shown to decrease the interphase area by 90% and more. This decrease is caused both by radial deflection of colliding droplets and loss of kinetic energy, which causes droplets to exit from the reactor sooner [an effect discussed by Elperin (1972) for solid particle flows in impinging streams reactors], and by coalescence, which reduces the surface area of droplets in the reactor. In collisionless flow, an increase in the nozzle separation distance results in an almost linear increase in interphase area, due to the linear increase in reactor volume and thereby in droplet holdup. In fact, the increase is steeper than linear, since an increase in H reduces the entrainment of droplets out of the reactor by decreasing the gas radial velocity (see [25]). The effect of collisions is shown in figure 6(a) to suppress this trend, with the interphase area attaining an asymptotic value for the large nozzle separation distance. This suppression is the result of the collision-induced screening effect of the droplets near the nozzle inlet, which prevents the buildup of droplet concentrations near the impingement zone.

In figure 6(c), the experimentally obtained dependence of $k_L A$ on the value of $2H$, for CO_2 absorption in flow conditions similar to those used in the study of Herskowits *et al.* (1988), is presented. The absorption rate is shown to initially increase with increased nozzle separation distance $2H$ and to remain eventually constant within $\pm$ 10%. Thus, the experimental results conform with the above prediction that droplet collisions curb the increase in the absorption rate with increased nozzle separation distance. However, within the range of relatively constant absorption rate with respect to H variation, the experimentally determined dependence displays one or two maxima in the absorption rate. These maxima in the absorption rate could not be discerned in the numerical simulation, as the magnitude of the relevant variations fells within the calculation error of at least 10–20% [referring to the spread in $\bar{A}$ values calculated for consecutive time periods, at steady state, and to the spread indicated in figure 6(a)]. Such maxima may be the result of additional factors relevant for relatively smaller values of H, when the screening effects are still weak. For instance, decreased droplet number densities, caused by increased reactor volumes, may reduce collision rates considerably and thereby increase the overall concentrations and surface area of droplets.

To examine the effect of turbulence on the absorber performance, the turbulent velocity pattern described above was employed in the calculation, the result being a decrease in the interphase area by about 50%, due to decreased droplet concentrations and enhanced coalescence. This is due to the effect of increased velocity differences between droplets, as indicated by [18], which increase collision rates. Still, since the exact gas turbulence pattern in the reactor is not known, the calculation performed above for laminar flow may be employed as an approximation of the real flow field.

9.2. Numerical analysis of combustion in impinging jets

The analysis of the effects of droplet collisions on pentane combustion in an impinging streams reactor was performed for a reactor with a 1.6 mm dia nozzle and a fuel feed rate (at each nozzle) of $F_L = 0.35$ g/s, for which an SMD of 35 μm has been reported by Faeth (1983). The gas was at a uniform temperature of 600 K and atmospheric pressure, and assumed to consist of 40% nitrogen on a molar basis, the rest being pentane vapour. Air was fed to each nozzle at a rate of $F_G = 0.008$ g/s. From these flow rates, the gas inlet velocity was estimated as $U_0 = 11.6$ m/s and the initial droplet volume fraction as $\beta_0 = 0.0076$. The calculation was performed for a minimal reactor diameter, $D_1 = 5$ mm. The initial droplet size distribution was identical to that used above for the absorption reactor, with the relevant SMD substituted as $\bar{\delta}$. The time increment in the simulation, Δt_m, had a value of 6.6×10^{-5} s, and values of the time-averaged vaporization rate in the reactor were determined over consecutive periods of $50\,\Delta t_m$. When droplet collisions were taken into account, the calculated values of the vaporization rate following 2–10 such intervals attained a constant value with an accuracy of 5–10%, and steady concentration patterns were obtained. In the absence of collisions, more droplets accumulated in the reactor and the steady-state condition was attained following 50–100 such periods. The overall steady-state numbers of droplets in the reactors, when droplet collisions were taken into account, were of the order of 5×10^5; values of the factorization factor k_f were in the range 10–40. A typical calculation consumed 8000 CPUs on a CDC Cyber 180/860 computer. The droplet population was discretized by dividing droplet diameters by $\delta_0/4$, where δ_0 indicates the Sauter mean diameter. Droplets with diameter $< \delta_0/5$ were not followed in the calculation.

In collisionless laminar flow, the effect of droplets accumulating near the reactor plane of symmetry due to the above mentioned effect of accumulation in a region of flow stagnation, was noticeable for low H values, but at higher $2H$ values this effect diminished due to the elimination of droplets by vaporization. The droplet size distribution shifted to lower diameter values downstream (see figure 7 for collisionless flow), due to vaporization. When collisions were taken into account with coalescence as the only collision outcome allowed, droplet number densities were higher near the nozzle than farther downstream, since coalescence and radial deflection by collisions prevented the buildup of high concentrations. Farther downstream, the size distribution widened and the maximum was shifted toward larger diameters (see figure 7). When fragmentation as a possible collision outcome was included, at high H values most droplets concentrated near the nozzle outlet, again due to vaporization and radial deflection and coalescence in collisions. Nevertheless, fragmentation by collisions caused many fragments to form downstream, so that for low H values, droplet number densities were largest near the reactor plane of symmetry, and for higher H values,

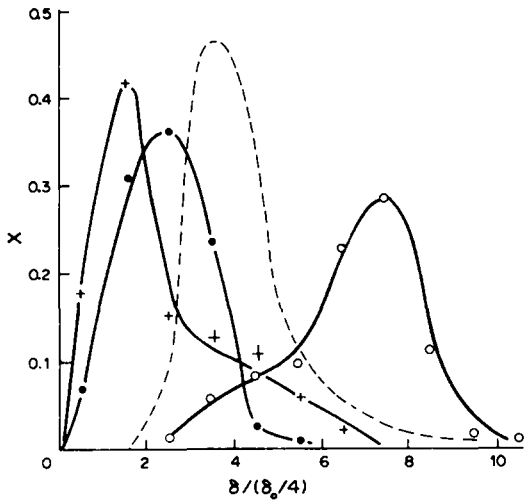

Figure 7. Calculated droplet size distributions in an impinging streams absorber,

$$X = \int_{r_{i-1}}^{r_i} dr \int_{\delta_{i-1}}^{\delta_i} d\delta f(\delta, r, t) \Big/ \left[\int_{r_{i-1}}^{r_i} dr \int_0^{\infty} d\delta f(\delta, r, t) \right]$$

($2H = 60$ mm). – – –, distribution at $z/H = 0.95$ for collisionless flow; ——, distributions at $z/H = 0.35$; ●, without collisions, ○, with collisions, only coalescence is accounted for; +, with collisions, fragmentation and coalescence are accounted for.

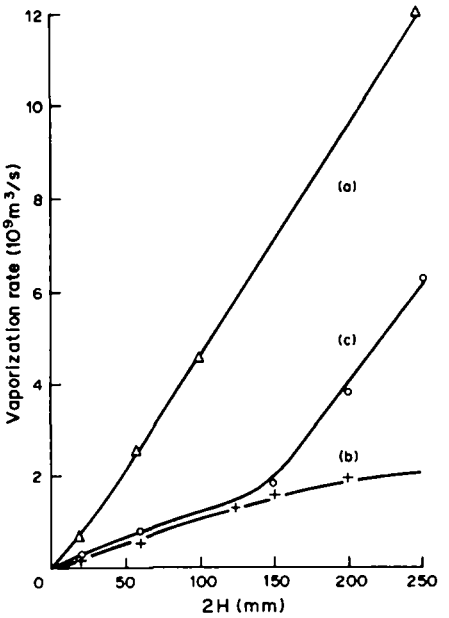

Figure 8. Calculated dependence of the average fuel vaporization rate on $2H$ for laminar flow in an impinging streams combustor. (a) Without collisions; (b) with collisions, only coalescence is accounted for; (c) with collisions, fragmentation and coalescence are accounted for.

droplet number densities were maximal at some intermediate location between the nozzle and the plane of symmetry. The obtained downstream size distribution (see figure 7) displayed a major decrease in the mean droplet size due to fragmentation. Coagulation was also significant, with a higher fraction of large droplets than in the case of collisionless flow.

In figure 8, the time-averaged overall vaporization rates calculated for (a) collisionless flow, (b) flow with only coalescence taken into account and (c) flow with both coalescence and fragmentation taken into account, are shown as a function of the nozzle separation distance, $2H$, in the reactor. Similar to absorption results, in the absence of collisions the vaporization rate increases almost linearly, due to the linear increase in reactor volume. Also, similarly, the droplet collisions when only coalescence is taken into account, caused a drastic decrease in the vaporization rate and a suppression of the increase in reactor performance when the nozzle separation distance was increased. When fragmentation by collision is also taken into account [figure 8(c)], the vaporization rate is still lower than that for collisionless flow, but higher than that obtained for coalescence only. The effect of fragmentation to increase the vaporization rate may be attributed to the increase in the interphase area for mass transfer. As H increases, the effect of fragmentation on the vaporization rate (with respect to the case of coalescence only) increases. The latter phenomenon may be due to several factors: (a) as H increases, droplet axial velocities increase in downstream flow (for a distance z' from the nozzle, the axial velocity found from [24] is $U_0[1 - z'/H]$), so that the collision frequency increases and, additionally, the probability for fragmentation by collision increases (see [1]); and (b) the effect of reduced droplet entrainment when increasing H is likely to cause more collisions than in the case of coalescence only, since retained fragments are of a wide spectrum of sizes, velocities and directions of motion.

Calculations were also performed for the flow of a low quality heavy fuel in air, corresponding to experiments performed by Elperin (1972) in an impinging streams combustor ($D_2 = 8.3$ mm, $H = 50$–70 mm, $\bar{\delta} \cong 300$ mm, $U_0 = 50$ m/s, $\rho_p = 990$ kg/m^3, $\mu_p = 0.0614$ kg/m s, $\sigma_p = 0.03$ kg/s^2). Results indicated that coalescence prevailed in the droplet interactions in this system, due to the high fuel viscosity.

10. CONCLUSIONS

The Monte Carlo method was developed to calculate the spatial variation of droplet size distributions in impinging dense fuel spray jets with droplet interactions. The developed numerical method may be applied to identify phenomena related to droplet interactions in other complex spray flows involving coagulation and fragmentation of liquid droplets.

For the impinging streams reactors, the suggested stochastic model and the DSMC procedure allow prediction of the spatial and size distributions of the liquid droplets and can be used to estimate optimal reactor volume, droplet residence time distributions etc.

While the hydrodynamic breakup of droplets in spray combustion has recently received much attention [see the review of Faeth (1987)], only a few works have mentioned the possible significance of the collision-induced breakup. The results presented in this work indicate that, for fuels of low viscosity and surface tension, the collision-induced breakup may significantly affect the droplet size distribution and flow pattern. Although the collision dynamics model employed in this work may not be sufficiently accurate to allow quantitative predictions of the structure of flows involving collision-induced breakup, the proposed method allows evaluation of the significance and possible effects of such breakup. One possible application is the analysis of dense sprays of low viscosity fuels in Bosch-type injectors for conventional spark-ignition engines (see Heywood 1988, pp. 294–299).

REFERENCES

Ashgriz, N. & Givi, P. 1987 Binary collision dynamics of fuel droplets. *Int. J. Heat Fluid Flow* **8,** 205–210.

Bajpai, R. K., Ramkrishna, D. & Prokop, A. 1988 A coalescence redispersion model for drop size distributions in an agitated vessel. *Chem. Engng Sci.* **31,** 913–920.

Best, A. C. 1950 Empirical formulae for the terminal velocity of water drops falling through the atmosphere. *Q. Jl R. met. Soc.* **76,** 302–311.

Bird, G. A. 1976 *Molecular Gas Dynamics.* Clarendon Press, Oxford.

Bird, R. B., Stewart, W. E. & Lightfoot, E. N. 1960 *Transport Phenomena.* Wiley, New York.

Borisov, A. A., Gelfand, B., Natanzon, M. S. & Kossov, O. M. 1981 Droplet breakup regimes and criteria for their existence. *J. Engng Phys.* **40,** 44–49.

Bradley, S. G. & Stow, C. D. 1979 On the production of satellite droplets during collisions between water drops falling in still air. *J. atmos. Sci.* **36,** 494–506.

Brazier-Smith, P. R., Jennings, S. G. & Lathan, J. 1972 The interaction of falling water drops: coalescence. *Proc. R. Soc.* **A326,** 398–408.

Brown, P. S. 1985 An implicit scheme for efficient solution of the coalescence/collision breakup equation. *J. comput. Phys.* **58,** 417–431.

Donaldson, C. D. & Snedecker, R. S. 1971 A study of free jet impingement. Part I. Mean properties of free and impinging jets. *J. Fluid Mech.* **45,** 281–319.

Donaldson, C. D., Snedecker, R. S. & Margolis, D. P. 1971 A study of free jet impingement. Part II. Free jet turbulent structure and impingement heat transfer. *J. Fluid Mech.* **45,** 477–512.

Elperin, I. T. 1961 Heat and mass transfer in impinging streams. *Inzh.-fiz. Zh.* **6,** 62 (in Russian).

Elperin, I. T. 1972 *Transport Processes in Impinging Jets.* Nauka i Tekhnika, Moscow (in Russian).

Faeth, G. M. 1983 Evaporation and combustion of sprays. *Prog. Energy Combust. Sci.* **9,** 1–76.

Faeth, G. M. 1987 Mixing, transport and combustion in sprays. *Prog. Energy & Combust. Sci.* **13,** 293–345.

Gelfand, F., Tambour, Y. & Seinfeld, J. H. 1980 Sectional representations for simulating aerosol dynamics. *J. Colloid Interface Sci.* **76,** 541–556.

Gillespie, D. T. 1975 An exact method for numerically simulating the stochastic coalescence process in a cloud. *J. atmos. Sci.* **32,** 1977–1989.

Gillespie, J. R. & List, R. 1979 Effects of collision-induced breakup on drop size distributions in steady state rainshafts. *Pure appl. Geophys.* **117,** 599–626.

Greenberg, J. B., Albagli, D. & Tambour, Y. 1986 An opposed jet quasi-monodisperse spray diffusion flame. *Combust. Sci. Technol.* **50,** 255–270.

HERSKOWITS, D., HERSKOWITS, V., STEPHAN, K. & TAMIR, A. 1988 Characterization of a two-phase impinging jets absorber—I. Physical absorption of CO_2 in water. *Chem. Engng Sci.* **43,** 2773–2780.

HETSRONI, G. 1982 *Handbook of Multiphase Systems.* Hemisphere, Washington, D.C.

HEYWOOD, J. B. 1988 *Internal Combustion Engine Fundamentals.* McGraw-Hill, New York.

KITRON, A., ELPERIN, T. & TAMIR, A. 1990 Monte Carlo simulation of gas–solids suspension flows in impinging streams reactors. *Int. J. Multiphase Flow* **16,** 1–17.

LANGMUIR, I. & BLODGET, K. 1948 Mathematical investigation of water droplet trajectories. *J. Met.* **5,** 175.

LEE, S. L. & WIESLER, M. A. 1987 Theory of transverse migration of particles in a turbulent two phase suspension flow due to turbulent diffusion—I. *Int. J. Multiphase Flow* **13,** 99–111.

LIFSHITZ, E. M. & PITAEVSKII, L. P. 1981 *Physical Kinetics.* Pergamon Press, Oxford.

MARSHALL, J. S. & PALMER, W. M. K. 1976 The distribution of raindrops with size. *J. met. Sci.* **5,** 165–166.

MCTAGGART-COWAN, J. D. & LIST, R. 1973 Collision and breakup of water drops at terminal velocity. *J. atmos. Sci.* **32,** 1401–1411.

MELVILLE, W. K. & BRAY, K. N. C. 1979 A model of the two phase turbulent jet. *Int. J. Heat Mass Transfer* **22,** 647–656.

MOSTAFA, A. A. & ELGHOBASHI, S. E. 1985 A two-equation turbulence model for jet flows laden with vaporizing droplets. *Int. J. Multiphase Flow* **11,** 515–533.

MOSTAFA, A. A. & MONGIA, H. C. 1987 On the modeling of turbulent evaporating sprays: Eulerian versus Lagrangian approach. *Int. J. Heat Mass Transfer* **30,** 2583–2593.

O'ROURKE, P. J. 1981 Collective drop effects on vaporizing liquid sprays. Ph.D. Thesis 1532-T, Dept of Mechanical & Aerospace Engineering, Princeton Univ., N.J.

PAI, S. I. 1974 Fundamental equations of a mixture of a gas and small spherical solid particles from simple kinetic theory. *Revue roum. Sci. Tech Mec. Appl.* **19,** 605–621.

PEARSON, H. J., VALIOULIS, I. A. & LIST, E. J. 1984 Monte Carlo simulation of coagulation in discrete particle-size distributions. I. Brownian motion and fluid shearing. *J. Fluid Mech.* **143,** 367–385.

PERRY, R. H. & CHILTON, C. H. 1973 *Chemical Engineers Handbook*, 5th edition. McGraw-Hill, Kogakusha.

PODVISOTSKY, A. M. & SHRAIBER, A. A. 1984 Coalescence and break-up of drops in two-phase flows. *Int. J. Multiphase Flow* **10,** 195–209.

PZUPPACHER, H. R. & KLETT, J. D. 1978 *Microphysics of Clouds and Precipitation.* Reidel, Dordrecht.

SAFFMAN, P. G. & TURNER, J. S. 1956 On the collision of drops in turbulent clouds. *J. Fluid Mech.* **1,** 16–30.

SIRIGNANO, W. A. 1983 Fuel droplet vaporization and spray combustion theory. *Prog. Energy Combust. Sci.* **9,** 291–322.

SOO, S. L. 1969 Pipe flow of suspensions. *Appl. scient. Res.* **21,** 68–84.

SOO, S. L. 1976 Net effect of pressure gradient on a sphere. *Phys. Fluids* **19,** 757.

TAMBOUR, Y. 1985a A Lagrangian sectional approach for simulating droplet size distribution of vaporizing fuel sprays in a turbulent jet. *Combust. Flame* **60,** 15–28.

TAMBOUR, Y. 1985b Coalescence of vaporizing kerosene fuel sprays in a turbulent jet. *Atomizn Spray Technol.* **1,** 125–146.

TAMIR, A. & KITRON, A. 1987 Applications of impinging streams in chemical engineering processes. *Chem. Engng Commun.* **50,** 241–330.